Contribution from the Inorganic Chemistry Laboratory, University of Oxford, South Parks Road, Oxford OX1 3QR, U.K., and University Chemical Laboratory, University of Cambridge, Lensfield Road, Cambridge CB2 1EW, U.K.

Kinetic Analysis of the Stereochemical Nonrigidity of the Triosmium μ_3-Arene/Alkene Complex $Os_3(CO)_8(\eta^2\text{-}CH_2CH_2)(\mu_3\text{:}\eta^2\text{:}\eta^2\text{:}\eta^2\text{-}C_6H_6)$ in the Solid State by ^{13}C CP/MAS NMR Spectroscopy

Stephen J. Heyes,[†] Mark A. Gallop,[‡] Brian F. G. Johnson,[‡] Jack Lewis,[‡] and Christopher M. Dobson*[,†]

Received January 3, 1991

A kinetic analysis of the ^{13}C CP/MAS NMR spectral line shapes of $Os_3(CO)_8(\eta^2\text{-}CH_2CH_2)(\mu_3\text{:}\eta^2\text{:}\eta^2\text{:}\eta^2\text{-}C_6H_6)$ in the temperature range 219–335 K indicates the existence of four of the five intramolecular dynamical processes observed for this molecule in solution. A jump-type reorientation of the benzene ring relative to the Os_3 cluster and Cramer-type rotation of the ethene ligand are shown to have activation energies in the solid state similar to those in solution, suggesting electronic control of such rearrangements. Ligand functionality interchange by a "turnstile" mechanism within the two different $Os(CO)_3$ sets is observed, but the relative rates show reversed ease of rearrangement in comparison to the case reported for solution. The trigonal twist process, which in solution interchanges the axial and equatorial carbonyls of the $Os(CO)_2(C_2H_4)$ group and transfers the ethene between equatorial sites, is not observed in the solid state, presumably because of crystal packing effects. Finally, the spectra at low temperatures show unexpected resonance multiplicities, which suggests the presence of different molecular conformers in the structure, which are dynamically interconverted at higher temperatures. These observations are rationalized in terms of general principles regarding the effects of intermolecular packing forces on processes concerning stereochemical nonrigidity. They also illustrate aspects of the general approach to extraction of kinetic data for dynamic processes from a line shape analysis of CP/MAS NMR spectra.

Introduction

Organometallic and metal cluster compounds show wide-ranging stereochemical nonrigidity, as determined primarily by solution-state NMR studies.[1,2] Particularly important in the kinetic and mechanistic elucidation of such processes has been line shape analysis of spectra in the exchange-broadened regime and latterly one- and two-dimensional magnetization transfer experiments in the slow limit, for which the line shapes are unaffected by the exchange process. It is of great interest to know whether the stereochemical nonrigidity of an organometallic compound, as identified by solution NMR studies, persists in the crystalline solid state and, if it does, to what extent the activation barriers for the various processes differ from those that pertain in solution. Until relatively recently information on molecular dynamical processes from solid-state NMR experiments was only possible through wide-line spectroscopy by the measurement of changes in the second moment or spin–lattice relaxation of the resonance with change in temperature. In this respect it has been shown recently that high-resolution, variable-temperature CP/MAS NMR spectroscopy is capable of producing spectra that enable the use of detailed line shape analysis and magnetization transfer techniques, thus providing detailed evidence for the existence of fluxionality and other dynamic processes in various organometallic compounds and also insight into the mechanistic and kinetic details.[3-15] We report here a variable-temperature ^{13}C CP/MAS NMR study of the metal cluster compound $Os_3(CO)_8(\eta^2\text{-}CH_2CH_2)(\mu_3\text{:}\eta^2\text{:}\eta^2\text{:}\eta^2\text{-}C_6H_6)$ (**1**), which contains an unusual bonding mode for benzene that caps a face of the triangular osmium cluster,[16] with the aim of determining the motional properties of this material in the solid state and comparing them to those in solution.

Extensive solution NMR studies of **1**, including variable-temperature ^1H and ^{13}C NMR and ^{13}C 2D-exchange spectroscopy, have shown that five independent fluxional processes may be detected.[18,19] With reference to the notation of Chart I, the Z/Z′/Z″ carbonyl ligands are permuted by a localized "turnstile" rotation that is not completely "frozen-out" even at 145 K and has a coalescence temperature of about 155 K. The Y/Y′/Y″ carbonyls are permuted by a similar, but higher energy process, with a coalescence temperature of 192 K. Steric hindrance to fluxionality from the greater proximity of the ethene ligand provides an explanation for the higher activation barrier for this process. The highest energy process interchanges, by a trigonal-twist pathway, the ligands of the $Os(CO)_2(C_2H_4)$ polytope,

Chart I. Molecular Structure and Notation for the Functionalities of **1**

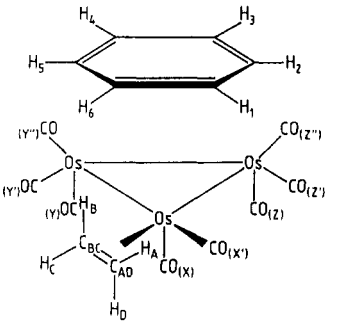

interchanging X and X′, the axial and equatorial carbonyls, with a coalescence temperature of 232 K, and effectively transferring

[†] University of Oxford.
[‡] University of Cambridge.

(1) Cotton, F. A. In *Dynamic Nuclear Magnetic Spectroscopy*; Jackman, L. M., Cotton, F. A., Eds.; Academic Press: New York, 1975; pp 377–440.
(2) Mann, B. E. In *Comprehensive Organometallic Chemistry*; Wilkinson, G., Stone, F. G. A., Abel, E. W., Eds.; Pergamon Press: Oxford, England, 1982; Vol. 3, pp 89–171.
(3) Dorn, H.; Hanson, B. E.; Motell, E. *Inorg. Chim. Acta* **1981**, *54*, L71–L73.
(4) Hanson, B. E.; Sullivan, M. J.; Davis, R. J. *J. Am. Chem. Soc.* **1984**, *106*, 251–253.
(5) Hanson, B. E.; Lisic, E. C.; Petty, J. T.; Iannaconne, G. A. *Inorg. Chem.* **1986**, *25*, 4062–4064.
(6) Hanson, B. E.; Lisic, E. C. *Inorg. Chem.* **1986**, *25*, 715–716.
(7) Wagner, G. W.; Hanson, B. E. *Inorg. Chem.* **1987**, *26*, 2019–2022.
(8) Hanson, B. E.; Whitmire, K. H. *J. Am. Chem. Soc.* **1990**, *112*, 974–977.
(9) Benn, R.; Grondey, H.; Nolte, R.; Erker, G. *Organometallics* **1988**, *7*, 777–778.
(10) Benn, R.; Mynott, R.; Topalavoič, I.; Scott, F. *Organometallics* **1989**, *8*, 2299–2305.
(11) Erker, G.; Sosna, F.; Peterson, J. L.; Benn, R.; Grondey, H. *Organometallics* **1990**, *9*, 2462–2467.
(12) Benn, R.; Grondey, H.; Erker, G.; Aul, R.; Nolte, R. *Organometallics* **1990**, *9*, 2493–2497.
(13) Heyes, S. J. D.Phil. Thesis, University of Oxford, 1989.
(14) Heyes, S. J.; Dobson, C. M. *J. Am. Chem. Soc.* **1991**, *113*, 463–469.
(15) Heyes, S. J.; Green, M. L. H.; Dobson, C. M. *Inorg. Chem.* **1991**, *30*, 1930–1937.
(16) The benzene ligation is best described as somewhere between the limiting descriptions of a bond-localized μ_3-cyclohexatriene and a completely delocalized μ_3-arene, bearing a striking resemblance to the Kekulé-type distortion found for benzene adsorbed on Rh(111) and Os(0001) single-crystal surfaces.[17]
(17) Gomez, M. P.; Johnson, B. F. G.; Lewis, J.; Raithby, P. R.; Wright, A. H. *J. Chem. Soc., Chem. Commun.* **1985**, 1682–1684.
(18) Gallop, M. A.; Johnson, B. F. G.; Keeler, J.; Lewis, J.; Heyes, S. J.; Dobson, C. M. *J. Am. Chem. Soc.*, in press.

0020-1669/91/1330-3850$02.50/0

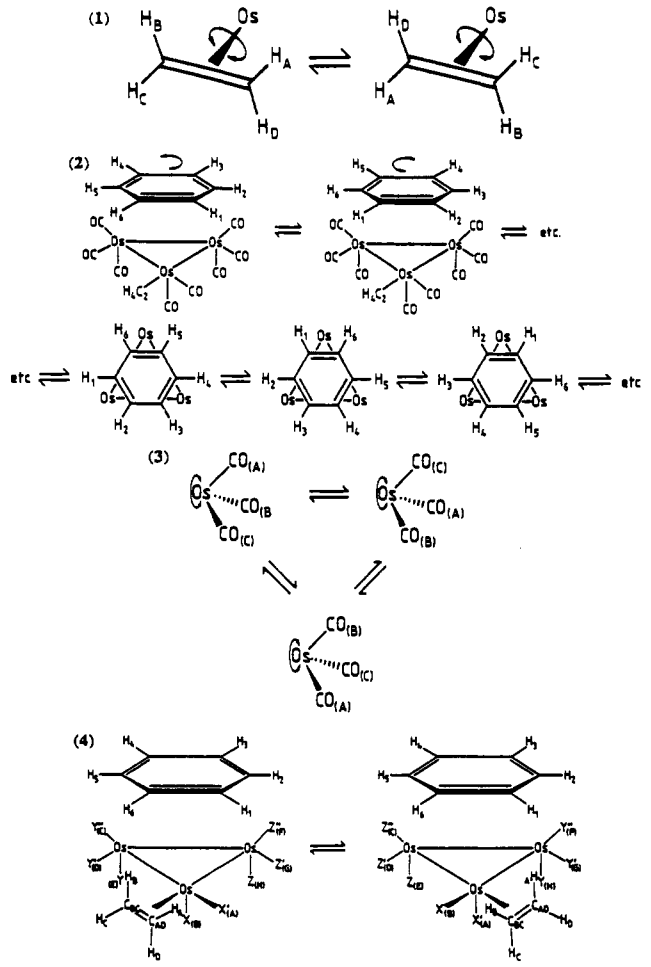

Figure 1. Schematic representation of the various types of fluxionality identified for $Os_3(CO)_8(\eta^2\text{-}CH_2CH_2)(\mu_3\text{:}\eta^2\text{:}\eta^2\text{:}\eta^2\text{-}C_6H_6)$ by the solution NMR studies of refs 17 and 18: (1) alkene reorientation; (2) two views of benzene ligand reorientation; (3) turnstile rotation of the $Os(CO)_3$ moieties; (4) the trigonal-twist process on the "front" $Os(C_2H_4)(CO)_2$ atom.

the alkene between equatorial sites. The above trigonal-twist process introduces a mirror plane of symmetry into the molecule and so removes the distinction between the Y and Z carbonyl sets. In addition to the effects of $Os(CO)_2(C_2H_4)$ polytopal rearrangement, a higher energy Cramer-type alkene rotation process about the Os–(C_2H_4) axis occurs. Finally, a 1,2-ring-hopping motion permutes the nuclei of the face-capping benzene ligand. All the fluxional processes were shown to be intramolecular, and the combined fluxional behavior has been described as "helicopter-like" motion. Of significance is the fact that the barrier for reorientation of the benzene moiety is considerably greater than that for site exchange of the alkene ligand; hence, the motions of the ring and alkene are **not** correlated. The various fluxional processes are shown in a schematic manner in Figure 1. We have shown separately in a qualitative analysis of ^{13}C CP/MAS NMR spectra that differences exist between the fluxional behavior of **1** in the solid state and in solution.[18] In this article we report the detailed manner in which the analysis of the solid-state ^{13}C CP/MAS NMR spectra has enabled a kinetic analysis of the various fluxional processes and has provided mechanistic insight into the dynamical properties of **1** in its crystalline form. We also discuss the more general implications of the observations from the solid-state NMR spectra.

Experimental Section

Preparative Methods. **1** was synthesized from $Os_3(CO)_9(\mu_3\text{:}\eta^2\text{:}\eta^2\text{:}\eta^2\text{-}C_6H_6)$[17] by reaction with trimethylamine *N*-oxide in acetonitrile and treatment of the resulting $[Os_3(CO)_8(NCCH_3)(\mu_3\text{:}\eta^2\text{:}\eta^2\text{:}\eta^2\text{-}C_6H_6)]$ in dichloromethane solution with ethene, using the procedure of ref 20. The sample of **1** was characterized by elemental analysis, infrared spectroscopy in a compressed KBr pellet, and extensive ^1H and ^{13}C solution NMR spectroscopy.

Solid-State NMR Spectroscopy. All solid-state NMR spectra were recorded on a Bruker CXP200 pulse NMR spectrometer with an Oxford Instruments 4.7-T wide-bore (98 mm) superconducting solenoid magnet (200.13 MHz for ^1H NMR) and equipped with an Aspect 2000 data system. ^{13}C CP/MAS NMR spectra were recorded at 50.32 MHz by using a multinuclear, proton-enhanced, double-bearing magic angle sample spinning probe (Bruker Z32-DR-MAS-7DB) and a high-power proton decoupler. A single contact spin-lock CP sequence[21] with alternate cycle spin temperature inversion, with flip back of ^1H magnetization,[22] and with a proton rf field of 1.7 mT (ω_1 = 72 kHz), resulting in a 90° pulse length of 3.5 μs, was used. Temperature regulation, utilizing a Bruker B-VT1000 unit equipped with a copper–constantan thermocouple and digital reference, was of the bearing gas and temperature measurement was of the bearing exhaust close to the sample. Temperature calibration below room temperature was achieved with the samarium ethanoate tetrahydrate Curie law chemical shift thermometer[23] previously calibrated against the phase transition of *d*-camphor[23] and above room temperature with the phase transitions of cobaltocenium hexafluorophosphate[24] and 1,4-diazabicyclo[2.2.2]octane.[23] The system was allowed to equilibrate at each new temperature for 1 h before spectral accumulation was commenced. The setting of the spinner angle was checked at each temperature by using the ^{79}Br resonance of a small amount of KBr,[25] separated from the sample by a plastic disk. Approximately 250 mg of a sample enriched to about 15% with ^{13}CO was packed into a 7-mm zirconia rotor with a Kel-F top. Spectra were recorded at temperatures from 219 K to 335 K at two MAS rotation rates, 4.25–4.5 kHz (depending on temperature) and ≈2.8 kHz. The spectral parameters, particularly the decoupler resonant frequency, the contact time, and the relaxation delay were optimized for the organic and carbonyl ligand regions of the spectrum in turn. Typically 1000–2000 transients, with a contact time of 2.5 ms and a relaxation delay of 3–15 s, were accumulated for each spectrum, in order to observe the resonances of the organic ligands, and up to 600 transients, with a contact time of 5 ms and a relaxation delay of 30–60 s, to observe the resonances of the carbonyl groups. Chemical shifts are reported on the δ scale with respect to δ(TMS) = 0 and were referenced to the secondary standard adamantane. The principal components of chemical shift tensors were recovered from the spinning-sideband manifold, measured in at least two slow spinning speed MAS NMR spectra,[26] using both the Maricq and Waugh moment analysis[27] and the Herzfeld and Berger graphical analysis.[28] Iterative comparison of the experimental and simulated[30] MAS NMR spectra was then used for refinement of the tensor components,[31,32] and such refined values are quoted with error limits derived

(19) Gallop, M. A.; Johnson, B. F. G.; Lewis, J.; Raithby, P. R. *J. Chem. Soc., Chem. Commun.* **1987**, 1809–1811.
(20) Gallop, M. A.; Housecroft, C. E.; Johnson, B. F. G.; Lewis, J.; Owen, S. M.; Raithby, P. R.; Wright, A. H. *J. Am. Chem. Soc.*, in press.
(21) Pines, A.; Gibby, M. G.; Waugh, J. S. *J. Chem. Phys.* **1973**, *59*, 569–590.
(22) Tegenfeld, J.; Haeberlen, U. *J. Magn. Reson.* **1986**, *69*, 191–195.
(23) Haw, J. F.; Campbell, G. C.; Crosby, R. C. *Anal. Chem.* **1986**, *58*, 3172–3177 and references therein.
(24) Heyes, S. J.; Clayden, N. J.; Dobson, C. M.; Wiseman, P. J. Unpublished results.
(25) Frye, J. S.; Maciel, G. E. *J. Magn. Reson.* **1982**, *48*, 125–131.
(26) The Herzfeld–Berger[28] convention for the labeling of sidebands is employed here. The conventional assignment for labeling of the principal components of the CSA tensor is used,[29] employing $\delta_{11} \geq \delta_{22} \geq \delta_{33}$ in order to indicate use of the δ chemical shift scale. The parameter $\Delta = (\delta_{11} - \delta_{33})$ is used as a measure of the spread of the CSA powder pattern and, together with the asymmetry parameter, $\eta = (\delta_{11} - \delta_{22})/(\delta_i - \delta_{33})$ if $(\delta_i - \delta_{33}) > (\delta_{11} - \delta_i)$, but $\delta = (\delta_{22} - \delta_{33})/(\delta_{11} - \delta_i)$ if $(\delta_i - \delta_{33}) < (\delta_{11} - \delta_i)$ (where $0 < \eta < 1$), characterizes any changes to the CSA caused by motional averaging.
(27) Maricq, M. M.; Waugh, J. S. *J. Chem. Phys.* **1979**, *70*, 3300–3316.
(28) Herzfeld, J.; Berger, A. E. *J. Chem. Phys.* **1980**, *73*, 6021–6030.
(29) Mehring, M. *Principles of High Resolution NMR in Solids*, 2nd ed.; Springer-Verlag: Berlin, 1983; pp 25–30.
(30) The MAS NMR spectrum at each MAS rate was simulated by using eq 30 of Maricq and Waugh[27,31] to evaluate the MAS FID from the tensor information. Powder averaging was performed in 2° steps, and the rotational echo was replicated to give 1024 points; the FID was convoluted with Gaussian and Lorentzian functions of choice and zero-filled to 8 or 16 K points.
(31) Clayden, N. J.; Dobson, C. M.; Lian, L.-Y.; Smith, D. J. *J. Magn. Reson.* **1986**, *69*, 476–487.
(32) As discussed in ref 31, the distinction between axial and near-axial tensors was not generally possible.

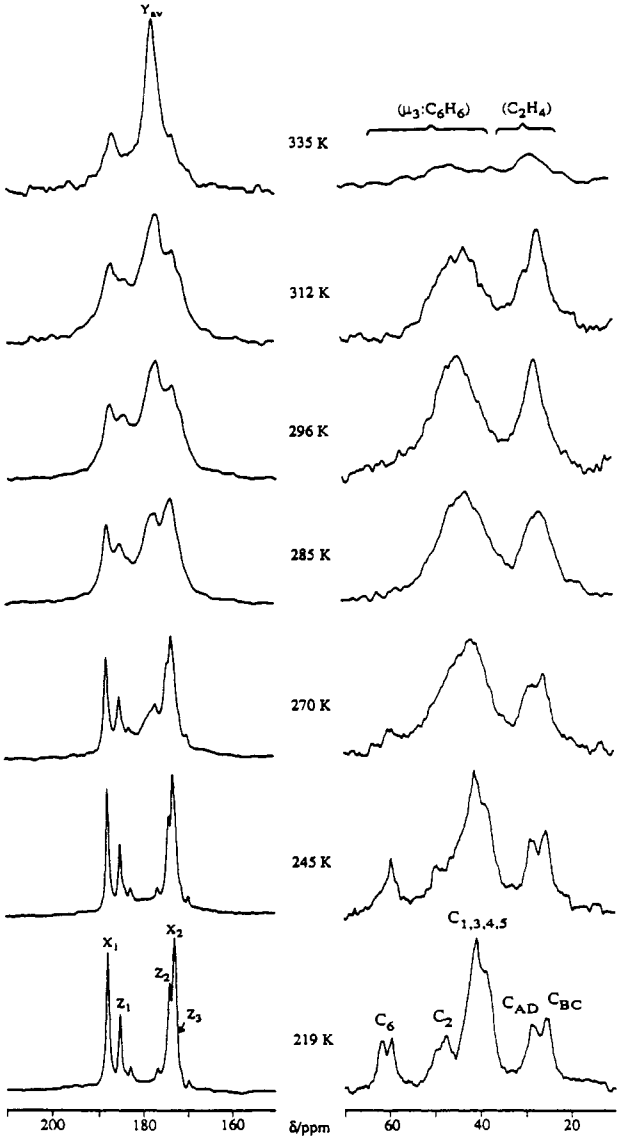

Figure 2. Isotropic regions of the ^{13}C CP/MAS NMR spectra of $Os_3(CO)_8(\eta^2\text{-}CH_2CH_2)(\mu_3{:}\eta^2{:}\eta^2{:}\eta^2\text{-}C_6H_6)$ (**1**).

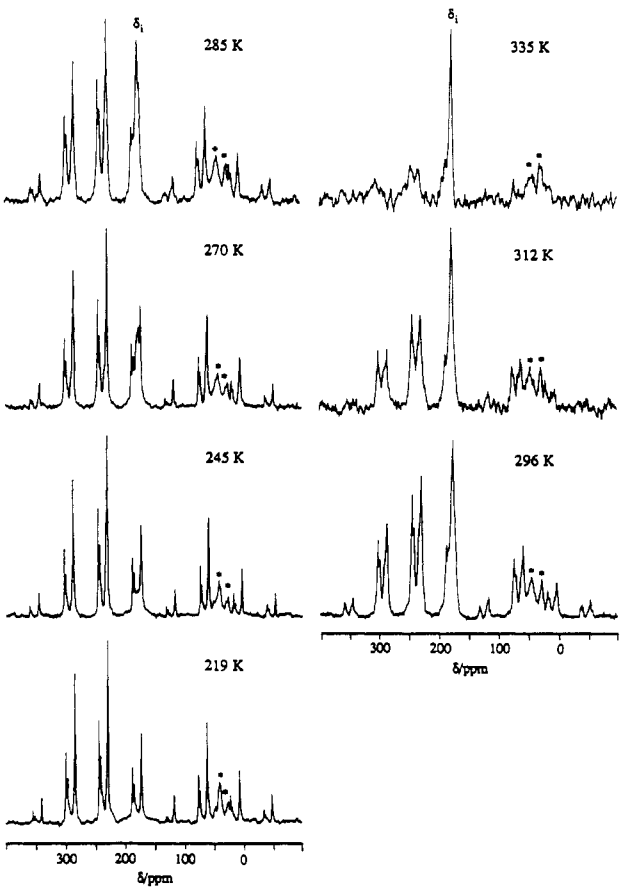

Figure 3. Full spinning-sideband ^{13}C CP/MAS NMR spectra for ^{13}C-enriched $Os_3(CO)_8(\eta^2\text{-}CH_2CH_2)(\mu_3{:}\eta^2{:}\eta^2{:}\eta^2\text{-}C_6H_6)$ (**1**), with MAS rate = ca. 2.8 kHz. Asterisks indicate peaks due to the organic ligands.

from the fitting process. The program DNMR4 (QCPE No. 466)[33] was used to calculate the exchange-broadened line shapes for coupled spin systems from the static (chemical shifts, coupling constants, and equilibrium populations of each of the accessible configurations of the system) and dynamic (relaxation and exchange matrices) input parameters in a full density matrix treatment.[34,35]

Results

(i) Variable-Temperature ^{13}C CP/MAS NMR Spectra. The ^{13}C CP/MAS NMR spectra of $Os_3(CO)_8(\eta^2\text{-}CH_2CH_2)(\mu_3{:}\eta^2{:}\eta^2{:}\eta^2\text{-}C_6H_6)$ (**1**) at temperatures from 220 to 335 K are shown in Figures 2 and 3. The resonances due to the benzene, ethene, and carbonyl ligands are clearly distinguishable from each other. The line shapes are temperature dependent and clearly indicate averaging of the low-temperature resonances with increasing temperature, implying that fluxional processes are operative in the solid state. All the line shape changes through the temperature range were found to be completely reversible.

Considering first the upfield region of Figure 2, as the temperature increases above 245 K, the resonances broaden and gradually coalesce within each of the benzene and ethene sets. Thus, at 296 K broad resonances centered at about 44.5 and 27.5 ppm are attributed to the partially time-averaged resonances of the six benzene and two ethene carbons, respectively. The coalescence temperature for the ethene ligand resonances is estimated as 275 K, from which a rate of two-site exchange of 330 Hz and an Eyring activation energy of $\Delta G_{275}^{\ddagger} = 54$ kJ mol^{-1} may be calculated. However, the new averaged resonances do not continue to sharpen with increase in temperature after coalescence, as expected for the passing of the exchange processes into the fast limit of the exchange-broadening time scale, but appear to be subject to further broadening from 270 to 335 K, at which temperature the resonances from the organic ligands are only just detectable. This difference between the solid-state and solution spectra arises because in solids the motional processes can interfere with interactions arising from specific aspects of the CP/MAS experiment other than just the exchange broadening due to averaging of the isotropic chemical shift. In particular, motion on the time scale of the magic angle sample spinning (MAS regime) may interfere with the averaging by MAS of the chemical shift anisotropy[36] and motion of the order of the frequency of the ^1H high-power rf decoupling field strength (ω_1) may interfere with the dipolar decoupling, and in both cases a region of broadening

(33) Bushweiler, C. H.; Letendre, L. J.; Brunelle, J. A.; Bilotsky, H. S.; Whalon, M. R.; Fleischmann, S. H. Quantum Chemistry Program Exchange Program, Program No. 466, DNMR4.
(34) Binsch, G. *Mol. Phys.* **1968**, *15*, 469–478.
(35) Binsch, G. *J. Am. Chem. Soc.* **1969**, *91*, 1304–1309.
(36) On moving from the coherent spatial averaging due to MAS in the strong collision limit to the incoherent averaging due to random molecular motion in the weak collision limit, the system should pass through an intermediate regime where the effects of molecular motion (correlation time τ_c) and MAS (rotation rate ω_r) interfere destructively leading to broadened NMR lines[37] (the maximum broadening from this effect is expected when $\sqrt{2}\omega_r\tau_c = 1$). In MAS NMR spectra the spinning-sideband intensities that reflect the CSA will also be affected by molecular motion in the MAS regime, though calculations based on the full sideband manifold are rather complex.[38]
(37) Suwelack, D.; Rothwell, W. P.; Waugh, J. S. *J. Chem. Phys.* **1980**, *73*, 2559–2569.
(38) Schmidt, A.; Smith, S. O.; Raleigh, D. P.; Roberts, J. E.; Griffin, R. G.; Vega, S. *J. Chem. Phys.* **1986**, *85*, 4248–4253.

Table I. ^{13}C CP/MAS NMR Data for the Carbonyl Region (Accessible Data)

	δ_i/ppm						$\Delta = (\delta_{11} - \delta_{33})$/
	solid	solution	δ_{11}/ppm	δ_{22}/ppm	δ_{33}/ppm	η	ppm
				219 K			
X_1	188.0	188.4	310 ± 10	310 ± 20	−60 ± 10	0	370
X_2	173.0	172.9	300 ± 10	300 ± 20	−80 ± 10	0	380
Z_1	185.2	185.3	310 ± 10	310 ± 20	−65 ± 10	0	375
Z_2	174.1	174.4					
Z_3	172.5	172.9					
				minor component			
Y_1	182.9	182.7					
Y_2	176.7	177.1					
Y_3	169.7	169.4					
				310 K			
X_1	188.0	188.4	310 ± 20	310 ± 25	−60 ± 25	0	375
X_2	173.5	172.9	305 ± 30	305 ± 30	−70 ± 30	0	375
Y_{av}	≈178	176.8	180 ± 40	180 ± 40	180 ± 40	1?	<80

is expected.[39] Due to the fairly small CSA of the organic ligands and the relatively high MAS speed employed (≈4.5 kHz), the broadening in the MAS regime will be of significantly smaller magnitude than the broadening in the dipolar decoupling regime (ω_1 = 72 kHz).

The initial broadening after coalescence is attributed to the ligand reorientation rates matching the MAS rotation rate. Especially noticeable is that the broadening of the exchange-averaged ethene resonance in the temperature range 280–330 K is considerably less severe than that of the averaged benzene ligand resonance. In the light of the differential broadening effects observed for two-site jumps of varying angular extent in the MAS regime,[37] the assumed ca. 180° jumps for ethene, which do not average the CSA, are not expected to cause major broadening, whereas the 60° "1,2" jumps likely to be preferred in benzene reorientation do average the CSA and are expected to cause large increases in line width. On decrease of the motional correlation time, before this source of line broadening becomes negligible, the broadening due to interference with the proton decoupling field becomes considerable and the experimental spectrum shows no distinct region of maximum broadening from the MAS effect. At the highest temperature studied, 335 K, maximum broadening has still not been reached,[41] but an estimate of ca. 360 K for the temperature at which the dipolar decoupling contribution to the line broadening peaks for both the benzene and ethene resonances leads to an estimated Eyring activation energy for the motions of $\Delta G_{\approx 360}^{\ddagger} \approx 55$ kJ mol^{-1}. This may be compared to the barriers of $\Delta G_{211}^{\ddagger} = 48.3 \pm 0.3$ kJ mol^{-1} for benzene reorientation and $\Delta G^{\ddagger} > 41$ kJ mol^{-1} for ethene rotation measured in solution.

On cooling from 245 to 220 K, however, multiple resonances become clearly resolved where only single resonances were observed in solution. Particularly clear are the cases for the C6 and C2 resonances of the benzene,[42] which show at least two discernible peaks and are spread over approximately 2–3 ppm. Also each of the ethene carbon resonances appears split into a doublet with a small separation (≈40 Hz) between the components. However, a one-to-one correspondence between magnetically distinguishable nuclei in solution and in the solid state would have been anticipated for **1**.[43] A possible explanation of these observations is that in the solid there may exist two or more NMR-distinguishable conformations of the molecule or part of the molecule.[44] These conformations presumably interchange either by action of the same processes responsible for the coalescence of the benzene and ethene resonances between 245 and 296 K or by a separate low-energy orientational interchange process, which is only frozen-out on the NMR time scale below 240 K.[45]

In the carbonyl region of the spectrum, at 219 K several sharp ($\Delta\nu_{1/2} < 30$ Hz) signals of varying intensities which appear to be superimposed on a very broad resonance are observed. CSA tensors were extracted from the intensity profiles of the spinning-sideband manifolds, showing the sharp resonances to have anisotropies consistent with those expected for static terminal carbonyl groups;[46,47] see Table I. The varying resonance intensities may be explained at least in part by differential cross polarization properties of carbonyls in different environments due to different coupling strengths to the proton spin bath.[48] On increase of temperature, by 270 K the broad component has started to emerge as a sharper resonance centered at 178 ppm. In addition, all the other carbonyl resonances are somewhat broadened at this temperature. This general broadening continues as the temperature is raised and has still not reached its maximum at 335 K. That this behavior is universal and that it coincides with the broadening of the benzene and ethene resonances strongly suggests that the general broadening regime is due to the dipolar broadening as the motion of the benzene and ethene ligands matches the frequency of the ^1H rf decoupling field.[40] The

(39) For a system in which ^{13}C spins are dipolar-coupled to ^1H spins experiencing an rf decoupling field of frequency ω_1, two ^{13}C NMR line-narrowing regions are predicted.[40] In the long correlation time limit, $\omega_1\tau_c \gg 1$, the line width, $\Delta\omega_{1/2} \propto \tau_c/\omega_1^2$, and in the short correlation time limit, $\omega_1\tau_c \ll 1$, $\Delta\omega_{1/2} \propto \tau_c$. The maximum broadening effect occurs when the motional and dipolar frequencies are equivalent (i.e. $\omega_1\tau_c = 1$).

(40) Rothwell, W. P.; Waugh, J. S. *J. Chem. Phys.* **1981**, *74*, 2721–2732.

(41) The dipolar broadening mechanism also explains the poor signal-to-noise ratio observed in the region of major broadening at 335 K, since on the matching of the motional and ^1H dipolar decoupling frequencies $T_{1\rho}(^1H)$ becomes very short, rendering the cross polarization process ineffective.

(42) The ring current shifts due to metal–ligand interactions are greatest for the benzene C6 and C2 resonances, which also show the largest resolved splittings.

(43) **1** has no molecular symmetry element other than the identity and occupies a general position within the space group $P2_1/n$ with one molecule per asymmetric unit.[19,20]

(44) Parsonage, N. G.; Staveley, L. A. K. *Disorder in Crystals*; OUP: Oxford, England, 1978.

(45) On the basis of the NMR results the mean atomic positions as determined in the room-temperature X-ray diffraction experiment would be expected to represent a time average of all possible atomic displacements, and this should be reflected in large thermal parameters. There is no evidence for irregularities among the thermal parameters for the ring or alkene carbons in the structure.[19,20] On the assumption that the space group and unit cell contents were correctly assigned in the diffraction study we note, however, that the large X-ray absorption corrections applied for the Os atoms in the refinement of the structure could mask the effects of any low-amplitude motions. Moreover, the marked anisotropies associated with the metal–ligand interactions in this complex suggest that even small ligand displacements might lead to the observed resonance splittings. The observations of separate coalescence of the C6 and of the C2 resonance "multiplets" on warming from 220 to 245 K prior to any significant exchange-broadening of the benzene ring carbons with each other and of coalescence of the ethene resonance pairs, which have a much smaller separation, only at 260 K suggests that the origins of the multiple resonances for the two different ligand types are separate. Presumably a crystallographic study at low temperature might detect two or more distinguishable orientations of the μ_3-benzene ligand relative to the basal Os_3 triangle, as outlined in ref 16 and likewise more than one orientation of the alkene ligand.[44]

(46) Gleeson, J. W.; Vaughan, R. W. *J. Chem. Phys.* **1983**, *78*, 5384–5392.

(47) Hasselbring, L.; Lamb, H.; Dybowski, C.; Gates, B.; Rheingold, A. *Inorg. Chim. Acta* **1987**, *127*, L49–L51.

(48) Yannoni, C. S. *Acc. Chem. Res.* **1982**, *15*, 201–208.

broadening of the carbonyl resonances is much less than for those of the organic ligands because the carbonyl carbon atoms are much further away from the protons. Further support is lent by the observation that all the resonances in the spectrum at 296 K are broader when recorded with a lower power of the ^1H decoupling field.

Direct chemical shift comparisons with the ^{13}C solution NMR spectrum at 145 K allows assignment of the resonances and analysis of the CP/MAS NMR spectra in terms of the three distinct "turnstile" rotations, which average the solution NMR spectra. The resonances at 174.1 and 185.2 ppm and the shoulder at 172.5 ppm, which appear eventually to coalesce at about 335 K ($\Delta G_{335}^{\ddagger} > 66$ kJ mol^{-1}), are assigned to the Z/Z′/Z″ carbonyl set. The broad resonance of the spectrum at 219 K, which continues to sharpen within the regime of general broadening of the carbonyl resonances, becomes the central resonance at 178 ppm in the spectrum at 312 K, which most noticeably has only a small CSA ($\Delta \ll 80$ ppm at 312 K), indicating that the carbonyls which it represents undergo an angularly extended reorientation. This resonance is assigned to the Y/Y′/Y″ set, which is evidently fluxional.[49] With the coalescence temperature estimated at 220 K ($T_c = 192$ K for the equivalent process in solution), an upper limit on the Eyring activation energy is set at $\Delta G_{220}^{\ddagger} < 44.5$ kJ mol^{-1}. Thus the Z/Z′/Z″ set can be seen to have a much larger activation barrier to interchange of ligands by turnstile rotation than the Y/Y′/Y″ set. This contrasts strongly with the behavior in solution where Z/Z′/Z″ ligand interchange is so facile it is not frozen-out even at 145 K. Thus, whereas in solution **intra**molecular factors, specifically the relative proximity of the bulky ethene ligand, must control the facility of carbonyl turnstile rotations, such that rearrangement within the Z/Z′/Z″ set is more facile than that within the Y/Y′/Y″ set, it appears that **inter**molecular "packing" effects are major factors in determining the equivalent barriers in the solid state. Consequently, the activation barriers are greater for motion of both ligand sets in the solid state, and the order of ease of rearrangement is reversed.[50] These values may be set in context by comparison with those derived for $M(CO)_3$ turnstile rotation in $M(C_6H_5Me)(CO)_3$, where for M = Cr $\Delta G^{\ddagger} = 65$ kJ mol^{-1} and for M = Mo $\Delta G^{\ddagger} = 70$–75 kJ mol^{-1}.[7] Finally, the resonances at 173 and 188 ppm, which remain relatively sharp at all temperatures and which crucially retain the large ^{13}C NMR CSA of a static terminal carbonyl even at higher temperatures ($\Delta \approx 370$ ppm at 312 K), are assigned to the X/X′ carbonyl set, showing that the trigonal-twist pathway, which interchanges axial and equatorial carbonyls and transfers the alkene between equatorial sites on the front Os atom, is a particularly high energy process in the solid state. This is consistent with the X-ray diffraction studies which do **not** support disorder of the ethene ligand between the two equatorial sites.[19,20] Thus, the only process that can average the alkene ^{13}C NMR resonances in the solid state is the Cramer-type alkene rotation, and the benzene resonances are not pairwise equilibrated by any ethene site averaging prior to the jump-type benzene reorientation process, as is the case in solution. This considerably simplifies the exchange pattern in the solid state and allows the possibility of a more thorough analysis of the line shape in the intermediate regime of the exchange-broadening time scale.

(ii) Kinetic Analysis. NMR exchange-broadened line shape simulations were compared with the experimental spectra for the cases of 1,2-jumps and random jumps of the benzene ring (the two extremes of the likely mechanism for the reorientation of this ligand) and also for the two-site exchange of the ethene and for the tricarbonyl turnstile rotations, giving rate data over a wider range of temperatures than possible merely by observation of coalescence or of the maximum broadening from the dipolar decoupling mechanism. The derived rates and Eyring free energies of activation are collected in Table II. The values of $\Delta G^{\ddagger} = 50$–54 kJ mol^{-1} for 1,2-hops and $\Delta G^{\ddagger} = 51.5$–$55$ kJ mol^{-1} for all site hops of the benzene ligand and of $\Delta G^{\ddagger} = 52$–55 kJ mol^{-1} for the ethene rotation are in reasonable agreement with the value of 55 kJ mol^{-1} suggested on the assumption of maximum broadening from the dipolar decoupling regime at 360 K and in the case of the ethene rotation with the value of 54 kJ mol^{-1} estimated from the simple two-site coalescence temperature. In the case of the turnstile reorientations of the tricarbonyl sets there are far less data available for the kinetic analysis. If the maximum broadening of the resonances of the Y set of carbonyls, which occurs at 230 K, is assumed to be due to coalescence in the exchange-broadening regime, line shape simulations show that $(1/\tau_c) \approx 400$ Hz implying that $\Delta G_{230}^{\ddagger} = 44.5$ kJ mol^{-1}. The broadening of the resonances of the Z set of the carbonyls with increase in temperature over and above the general broadening of the carbonyl resonances due to the dipolar decoupling mechanism is assumed to be due to turnstile rotation, and the exchange-broadened line shapes could be simulated, leading to values of $\Delta G^{\ddagger} = 64$–65 kJ mol^{-1}, clearly significantly higher than the value of $\Delta G^{\ddagger} \approx 44$ kJ mol^{-1} obtained for the turnstile reorientation of the Y carbonyl set.

Line shape analysis providing rate data over a range of temperatures enables determination of kinetic activation parameters for the various possible fluxional processes. Best-fit Arrhenius

Table II. Rate Data for Processes of Stereochemical Nonrigidity As Determined from the ^{13}C CP/MAS NMR Spectra[a,b]

Temperature/K	$1/\tau_c$(est.)/s^{-1}	$\Delta G^{\ddagger}_T$/kJmol^{-1}
Ethene Reorientation		
Exchange Broadening		
296	1000*	55.5
285	500*	55
275	330	54
270	250	53.5
245	60	51.5
Arrhenius Parameters: $E_a = 35.5$ kJmol^{-1}		$A = 2.0 \times 10^9$ s^{-1}
Maximum Dipolar Broadening		
335 (360)	71500	51 (55)
Benzene Reorientation		
Temperature/K	$1/\tau_c$(est.)/s^{-1}	$\Delta G^{\ddagger}_T$/kJmol^{-1}
(a) by 1,2 hops		
Exchange Broadening		
296	2000*	54
285	1250*	53
270	550	52
245	175	49
Arrhenius Parameters: $E_a = 31$ kJmol^{-1}		$A = 6.2 \times 10^8$ s^{-1}
Maximum Dipolar Broadening		
335 (360)	71500	51 (55)
(b) by all-site hops		
Exchange Broadening		
296	850*	56
285	450*	55
270	250	53.5
245	75	51
Arrhenius Parameters: $E_a = 30$ kJmol^{-1}		$A = 1.8 \times 10^8$ s^{-1}
Maximum Dipolar Broadening		
335 (360)	71500	51 (55)

[a] The rate data for the exchange broadened spectra were obtained by using the program DNMR4. The rate data at 335 K (360 K) were obtained by assuming this to be the temperature of maximum broadening on the dipolar broadening time scale for all resonances and all pertinent reorientational mechanisms, though it is by no means certain that this is the case, and the maximum dipolar broadening temperature might be considerably higher. However, note the general agreement of derived kinetic data. [b] Asterisks indicate data corrected for dipolar broadening effects as explained in the text.

(49) At 219 K very low intensity, sharp, resonances are seen at 169.7, 176.7, and 182.9 ppm. On comparison with the solution NMR data, these are very close to the shifts expected for a static Y/Y′/Y″ set. These resonances have extended spinning sideband manifolds consistent with a static nature, and remain relatively sharp until 270 K above which the general broadening of the carbonyl resonances renders them unobservable. Their relative intensity is not increased by alteration of the cross polarization conditions or of the recycle delay. They could be due to a minor crystalline form of **1** in which the Y/Y′/Y″ set is not fluxional.

(50) This correlates with the distances to the nearest neighbouring protons suggested by the facility of cross polarization to ^{13}C, as reflected in the ^{13}C NMR intensity of the various carbonyl resonances.

Table III. Comparison of Dynamic Properties of **1** in the Solid State and in Solution

	solution	solid state
benzene 1,2-hops	$\Delta G_{211}^{\ddagger} = 48.3$ kJ mol^{-1}	$\Delta G^{\ddagger} = 49$–54 kJ mol^{-1}
ethene rotation	$\Delta G^{\ddagger} > 41$ kJ mol^{-1}	$\Delta G^{\ddagger} = 51$–55.5 kJ mol^{-1}
CO's turnstile rotation		
Z set	$T_c = 192$ K	$\Delta G^{\ddagger} > 66$ kJ mol^{-1}
Y set	$T_c = 155$ K	$\Delta G^{\ddagger} < 44$ kJ mol^{-1}
front Os trigonal twist: *X* set	$\Delta G^{\ddagger} = 40.5$ kJ mol^{-1}	not obsd in the solid
conformational averaging process		lower energy process than benzene or ethene reorientation

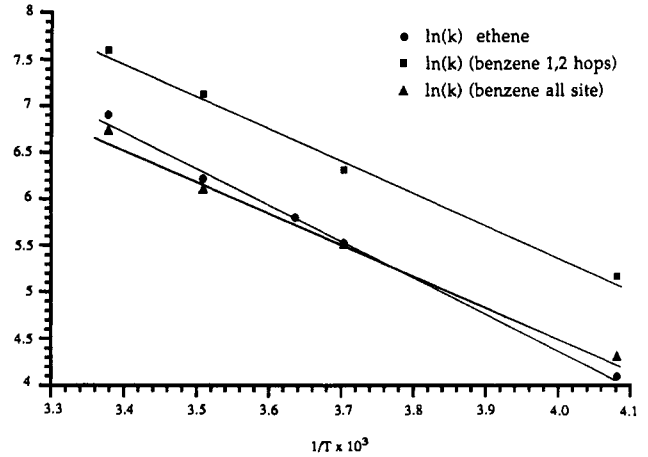

Figure 4. Plots of ln k versus $1/T$ from the fitting of the exchange-broadened line shapes for (a) ethene reorientation, (b) benzene reorientation by 1,2-hops, and (c) benzene reorientation by all-site hops, showing the best-fit Arrhenius parameters.

activation parameters, determined as shown in Figure 4, are $E_a = 31$ kJ mol^{-1} with $A = 6.2 \times 10^8$ s^{-1} for 1,2-hops or $E_a = 30$ kJ mol^{-1} with $A = 1.8 \times 10^8$ s^{-1} for all-site hops of the benzene ligand and $E_a = 35.5$ kJ mol^{-1} with $A = 2.0 \times 10^9$ s^{-1} for the ethene reorientation. The rates indicated on the basis of the simple exchange-broadened line shape simulations for these processes in the higher temperature regime (>275 K) are generally lower than expected on the bases of these Arrhenius relationships as presented. This is assumed to be due to a failure to take into account the spectral broadening present as the rates of motion reach the MAS and dipolar decoupling regimes. Table II shows rate values at 285 and 296 K, corrected for the effects of the dipolar broadening mechanism. The broadening expected for the ethene/benzene resonances was derived from the broadening actually observed for the resonances of the carbonyl "X" set at the same temperatures by utilizing a simple distance ratio model (r'^6/r^6) to scale the dipolar decoupling contribution. The corrected values fit the Arrhenius relationships much better, though still underestimating the rates of the reorientation processes slightly. The derived Arrhenius activation energies are similar to values obtained for similar processes in solution, thus indicating little effect from the crystalline environment on the energetics of either reorientation process. It is not ascertainable from the NMR data, though, whether the similarity in activation barriers for the benzene and ethene reorientational processes in the solid state means that the motions are positively correlated ("geared") in any way.

In summary, of the five dynamic processes detected in the NMR spectra of **1** in solution, four still prevail in the solid state, and a new dynamic process, which equilibrates conformational isomers, whose kinetic analysis is evidently not accessible in solution, is detected in the solid state. A synoptic comparison of the processes in the two environments is presented in Table III.

(iii) Discussion. The results of the study described in this paper illustrate clearly a number of features relating to the extraction of kinetic data for dynamic processes from CP/MAS NMR spectra. For processes that involve exchange between sites with resonance positions separated by less than ca. 2000 Hz, or greater for systems with small chemical shift anisotropy, the line shape profile of the isotropic resonances may be simulated on the basis of exchange-broadening. Generally the resonances in CP/MAS NMR spectra are broader than those in solution NMR studies, and in cases such as **1**, where resonance overlap is considerable, this limits the accuracy with which the line shapes may be fitted. The derived activation energies, E_a, are, however, usually accurate, though preexponential factors, A, may be less trustworthy. Here as in most cases,[7,13,14] however, the averaged resonances do not sharpen into the fast limit of the exchange-broadening time scale, due to the extra sources of broadening in the MAS and dipolar decoupling regimes, and indeed these sources of broadening are usually significant over a rather large temperature range for CP/MAS NMR spectra run under standard conditions. These broadening processes, which clearly have no solution NMR equivalent, potentially provide extra rate information, allowing the kinetic analysis to be extended to shorter correlation times. However, in such complex systems as **1** it generally proves impossible to deconvolute accurately the various contributions to the line broadening, and indeed with the MAS rates (2–20 kHz) and decoupling field strengths generally used in CP/MAS NMR ($\omega_1 \approx 30$–100 kHz) a distinct region of maximum broadening due to the MAS regime is generally not observed, because of continuing broadening from the dipolar decoupling mechanism. In **1**, therefore, it proved, as has been the case in most other systems studied by CP/MAS NMR to date, possible only to estimate the free energy of activation from identification of the temperature of maximum broadening due to the dipolar decoupling mechanism. While this work illustrates the possibility of "solution-like" isotropic chemical shift analysis of dynamic processes in solids by CP/MAS NMR spectroscopy, also of great importance has been the analysis of chemical shift anisotropy data, a source of information unavailable in solution.

It has been suggested very recently from the results of atom–atom potential energy calculations[51] that tricarbonyl rotation in the $Os(CO)_3$ groups of **1** appears to be totally prevented by molecular packing and that large amplitude torsions of the $Os(CO)_3$ groups could be the cause of our NMR observations. However, the coalescence of the NMR isotropic shifts to a single averaged peak and also the extensive averaging of the chemical shift anisotropy of the Y and Z carbonyl resonances cannot in fact be produced by even large amplitude oscillations, which would in any case be expected to occur on a much shorter time scale than the motions detected in these ^{13}C CP/MAS NMR spectra. The information obtained from the measurement of the CSA is a particular feature of NMR in the solid state that may often provide conclusive evidence in favor of occurrence of a particular dynamic process. In this case the observed extensive averaging of the CSA is equivalent to that expected from a $M(CO)_3$ turnstile reorientation process. We conclude that turnstile reorientation is the only process that can satisfactorily explain all the solid-state NMR evidence. A possible reason for this anomaly is that the potential energy calculations do not take account of relaxation in the local intra- and intermolecular environment of the tricarbonyl set as reorientation occurs. The observation of reorientation by NMR shows that such relaxation must have substantial influence in facilitating such a process and may even indicate that

(51) Braga, D.; Grepioni, F.; Johnson, B. F. G.; Lewis, J.; Martinelli, M. *J. Chem. Soc., Dalton Trans.* **1990**, 1847–1852.

$Os(CO)_3$ turnstile reorientation can only occur by virtue of cooperative effects in the crystal lattice.

The observations described in this paper, coupled with those of previous studies,[3-15] suggest some generalizations concerning the comparison of dynamic processes in solution and in the solid state. It might be imagined that placing a molecule in a crystal lattice may influence the fluxional processes of an isolated molecule in several distinct ways, and the evidence presented in this work allows for the discussion of these various possibilities. First, some low-energy processes are observed in solids, which are not detected in solution NMR, because they are always "fast" on the NMR time scale in solution. For example for **1** we observed an unexpected dynamic interchange process, involving the benzene and ethene ligands, between at least two different molecular conformers in the solid-state structure. Such processes may well be more common than expected from examination of solution NMR spectra, in which they are always rapid on the NMR time scale, and crystallographic data, in which they may show up as disorder, but perhaps not always of sufficient amplitude to be detected.

The activation barriers to some dynamic processes, the benzene and ethene ligand reorientations in **1** are examples, appear to be very similar in solution and in the solid state. This may be interpreted as meaning that such processes are controlled primarily by electronic factors involved in the rearrangement of valence electrons, compared to which steric effects, both *intra-* and *inter*molecular, are insignificant. However, sterically demanding processes such as the trigonal-twist process of the $Os(C_2H_4)(CO)_2$ group in **1** may be prevented from occurring by the molecular packing characteristics. In such cases we may imagine that *inter*molecular steric effects, due to the specific packing arrangement, that act directly on the group or groups involved in the potential dynamic process are the cause of the increased barrier to motion in the crystalline state. For other processes, for which the relative facility of motion in a solution environment is principally determined by *intra*molecular steric effects, the *inter*molecular packing effects of the crystalline state may be regarded as influencing the situation in two ways. In the first place, as discussed above, there are direct *inter*molecular steric effects acting on the potentially motional groups. The additional factor of *inter*molecular steric effects leads to such processes having larger activation barriers in the crystalline state than in solution. Second, the *inter*molecular steric effects on other groups of a molecule may modify the *intra*molecular steric forces acting within the molecule and ultimately influence the activation barrier to a fluxional process. There are two ways in which this might be conceived. First, the *inter*molecular steric effects could cause molecular conformational differences in the crystalline state compared to the situation in solution and so directly modify the *intra*molecular steric forces. Second, the facility of dynamic processes within a molecule is likely to be enhanced by relatively large amplitude vibrations of surrounding groups, which allow relaxation of the structure around the mobile functionality as the dynamic process occurs. Specific *inter*molecular interactions in the crystalline state may reduce the ability of the surrounding groups to relax around the mobile group and so increase the activation barrier to the dynamic process. This is illustrated by the reversal in the solid state relative to solution of the order of facility of the turnstile reorientations of the $Os(CO)_3$ functionalities of **1**, control of these processes in the solid state is likely to be due to **inter**molecular steric effects acting both directly and also indirectly by influencing **intra**molecular effects.

Registry No. $Os_3(CO)_8(\eta^2\text{-}CH_2CH_2)(\mu_3\text{:}\eta^2\text{:}\eta^2\text{:}\eta^2\text{-}C_6H_6)$, 118772-73-9; Os, 7440-04-2.

Contribution from the Departments of Chemistry, Northwestern University, Evanston, Illinois 60208, and University of San Francisco, Ignatian Heights, San Francisco, California 94117

Solvent-Induced and Polyether-Ligand-Induced Redox Isomerization within an Asymmetrically Coordinated Mixed-Valence Ion: *trans*-$(py)(NH_3)_4Ru(4\text{-}NCpy)Ru(2,2'\text{-}bpy)_2Cl^{4+}$

Jeff C. Curtis,*[†] Jody A. Roberts,[‡] Robert L. Blackbourn,[‡] Yuhua Dong,[‡] Mohammed Massum,[†] Christopher S. Johnson,[‡] and Joseph T. Hupp*[‡]

Received February 27, 1990

Advantage is taken of oxidation-state-dependent ligand (ammine)/solvent interactions to shift redox potentials and effect redox isomerization in the title complex. In poorly basic solvents, the stable isomeric form is *trans*-$(py)(NH_3)_4Ru^{II}(NCpy)Ru^{III}(bpy)_2Cl^{4+}$ (py is pyridine; NCpy is 4-cyanopyridine; bpy is 2,2'-bipyridine). In contrast, in stronger Lewis bases or in a mixture of strong and weak bases (dimethyl sulfoxide + nitromethane), the preferred isomer is *trans*-$(py)(NH_3)_4Ru^{III}(NCpy)Ru^{II}(bpy)Cl^{4+}$. Evidence for redox isomerization was obtained, in part, from plots of formal potentials versus solvent Lewis basicity. Confirmatory evidence was obtained from a combination of electrochemical reaction entropy and resonance Raman spectroscopic experiments. UV-vis-near-IR absorption experiments, however, were not found to be useful in demonstrating isomerization. In a related series of experiments, redox isomerization was also demonstrated based on ammine binding by either a low molecular weight poly(ethylene glycol) species or by a macrocyclic ligand, dibenzo-36-crown-12. Much smaller molar amounts of either the polymer (substoichiometric) or crown (approximately stoichiometric) are required, in comparison to basic solvent (severalfold excess), in order to induce isomerization in nitromethane as the initial solvent. The possible general utility of the redox isomerization concept in time-resolved intramolecular charge-transfer studies and in optical studies of competitive hole- and electron-transfer pathways is mentioned.

Introduction

A few years ago we reported on the first example of solvent-induced redox isomerization in a mixed-valence system.[1,2] The system of interest was the symmetrically bridged, heteronuclear bimetallic complex, $(bpy)_2ClOs(pyrazine)Ru(NH_3)_5^{4+}$ (bpy is 2,2'-bipyridine). The basis for isomerization was in the overall energetic proximity of the Os(III/II) and Ru(III/II) formal potentials (E_f) and in the marked solvent tunability of the latter. For this system the oxidation state distribution was found to be

[†] University of San Francisco.
[‡] Northwestern University.

(1) Hupp, J. T.; Neyhart, G. A.; Meyer, T. J. *J. Am. Chem. Soc.* **1986**, *108*, 5349.
(2) Related reports: (a) Neyhart, G. A.; Meyer, T. J. *Inorg. Chem.* **1986**, *25*, 4808. (b) Olabe, J. A.; Haim, A. *Inorg. Chem.* **1989**, *28*, 3277.

0020-1669/91/1330-3856$02.50/0